Shahid Chamran University of Ahvaz
Irrigation Sciences and Engineering (JISE) Vol. 43, No. 4, Winter 2021, Original Paper p. 91-104

Laboratory investigation of deflector structure effect on bridge pier scouring

Mohsen Solimani Babarsad[1*], Amin Hojatkhah[2], Abbas Safaei[3] and Roozbeh Aghamajidi[4]

1*- Corresponding Author, Department of Water Sciences,Water Science and Environmental Research Center, Shoushtar Branch, Islamic Azad University, Shoushtar, Iran. *(Mohsen.solb@gmail.com).*
2- Water Science and Environmental Research Center, Shoushtar Branch, Islamic Azad University, Shoushtar, Iran.
3- Water Science and Environmental Research Center, Shoushtar Branch, Islamic Azad University, Shoushtar, Iran.
4- Assistant Professor civil department, Islamic Azad University, Sepidan Branch, Sepidan, Iran.

Received: 9 January 2021 Revised: 18 February 2021 Accepted: 21 February 2021

Abstract
Bridge pier local scouring is a crucial factor in bridge destruction. Studies from different researchers have presented solutions to control this phenomenon. These solutions are divided into two parts, namely, direct and indirect protection. In the direct method, the bed is armoured against scouring whereas in the indirect methods the flow pattern around the pier is changed with geometric parameters. This study defined an element called the deflector structure (flow diverter) to divert the bed's flow streamline in front of the pier. Experimental scenarios were defined by stabilizing the flow conditions with 0.70, 0.83, and 0.97 relative velocities (U/U_c) and 15-, 30-, and 45-degree wedge deflector structure angles with flow direction for two piers with square and circular cross-sections. The results showed that the dimensionless scour depth parameter (d_s/d) close to the particle movement threshold ($U/U_c = 0.97$) was reduced by 70 to 75%, respectively relative to the control model for square and circle cross-section. Changing the angle from 45 to 30 and 15 degrees reduces the local pier scouring and increases the deflector structure's effectiveness.

Keywords: Bridge pier, Deflector, Flow diverter, Local scour, Movement threshold.
DOI: 10.22055/jise.2021.36337.1950.

Introduction

Bridge collapses due to scour is an important socio-economic problem that has been the subject of numerous studies over the past decades. Bridge destruction due to scour has motivated researchers to study the subject and present modern methods for its control and reduction. Scour is particles whcih transfer from their original position to another caused by the flow shear stress. Local scour is divided into two types, namely 1- Clear-water scour and 2- Live-bed scour. Local scour depth reduction methods are divided into the following two categories: 1- Bed material armouring using rigid materials, the most common being river bed pitching, and 2. weakening the main bed erosion factors and changing the flow pattern contacting the pier. The tools for this method include using the sill, submerged vanes, slots, collars, and deflector structures, or using secondary tools that generally change the vortex pattern around the pier.

The scour mechanism around the bridge pier

Common factors of bridge pier scour include down flows, horseshoe vortexes, and wake vortexes. In general, the impact of flow on the pier and its separation are the main factors that form scour holes around piers.

Researchers, including Choramin et al. (2015), Akhlaghi et al. (2020), Wang et al. (2020), and Adib et al. (2019) have published numerous studies on the flow pattern around the bridge piers. The horseshoe vortex is the

most important scour hole factor. As the water flow impacts the pier, the velocity gradient changes into the pressure gradient due to velocity reduction as a result of the flow affecting the pier face. Simultaneously, the velocity reduction from the surface to bed reduces the dynamic pressure on the pier from top to bottom. The pressure gradient creates a down flow toward the bed that digs the sedimentary bed and disperses sediments around the pier (Raudkivi, 1998). Down flow returns up and is forced to stream in the flow direction after joining the main flow. This rotation and return of the flow creates the horseshoe vortex around the pier (Kayatürk, 2005). The horseshoe vortex around the scour hole accelerates digging and transfers the sediments separated from the bed downstream with the main flow. The flow's separation from around the pier also creates perpendicular vortexes on the sedimentary bed known as wake vortexes. These vortexes are active behind the pier, separate the bed particles like a tornado, expose them to the flow, and help move sedimentary particles from the front and sides of piers downstream. The scour hole digging by the horseshoe vortex continues until the water volume inside the scour hole is increased, thereby exhausting the energy of the vortex. In this state, the scour depth changes negligibly over time and reaches equilibrium. Figure (1) show the scour mechanism.

Researchers have also studied the weakening of the main bed's erosion criteria and changing the flow pattern. The literature on the pier bed protection is presented as follows.

Zomorodian et al. (2019) evaluated the separate and combined effects of sacrificial piles and collars in the local scour on the bridge pier group with square collars. In this study, the scour depth was reduced by 69.23% in the front pier, 63.23% in the middle pier, and 67.7% in the back pier. They also observed that using sacrificial piles provides stronger protection in the front pier, and that combining the two methods results in scour equilibrium and improvement in all three beds relative to different ways. Shahsavari et al. (2019) investigated the effect of semi-circular collar placement on the bridge abutment scour depth and flow pattern. They conducted their experiments in clear-water and semi-circular collars on L1.5 and L2 (length of support against the flow) semi-circular abutments, and three different levels (at bed level, and 0.2L below and above it). Their results showed that the collar with double support length (L2) and placement level (0.2L) under the bed performed better and reduced the final scour depth by 58%. Also, Raeisi and Ghomeshi (2020) investigated the flow and the scour pattern around the bridge pier with an asymmetrical mesh collar. The asymmetrical collars were used at three different heights (on the bed, and 1 cm and 2 cm above the bed), with 15, 30 and 40% mesh percentages, and the best mesh collar efficiency was observed at the 1 cm level above the sedimentary bed. They were corresponding to the 15% mesh collars that achieved a 44% decrease relative to the control experiment. The results also suggested that the 40% mesh collar reduced scour more than the 30% mesh collar. Nohani and Ebrahimi (2019) conducted laboratory analysis of the collar and submerged vanes on decreasing scour depth in bridges with cylindrical piers and three collar diameters, 2, 4 and 6 submerged vanes, and at the 45-degree angle. According to the results, the D_2 collar diameter and the six submerged vanes resulted in the maximum scour depth decrease of 98%. Vaghefi and Meraji (2019) analysed the effect of the 20% upstream submerged vale overlap reduction on the bridge pier on 180° sharp curve bed topography. The results showed that the 20% submerged vane overlap reduction also decreased the scour depth by 30%. Abousaeidi et al. (2018) investigated the effect of floating objects on the pier and abutment local scour and the interaction between the bridge abutment and pier and thickness, effective length, and shape of the floating objects. The results indicated that the scour depth was directly correlated with the relative thickness of the floating objects, and that doubling the relative thickness of rectangular floating objects increased the abutment and pier local scour by 1.2 and 1.05. Gohari and Rezaei (2020) studied the effect of oblique sill on bridge pier scour with circular cross-sections. The oblique sill was investigated diagonally at 11.3 degrees relative to the wall in contacting and longer proximities from the

 DOI: 10.22055/jise.2021.36337.1950.

pier. They concluded that increasing the sill to pier distance reduces its protective effect. The best results corresponded to the oblique sill attached to the L=0 pier, and the oblique sill decreased further than the bed sill, volume, and maximum scour depth. After reviewing the literature on sacrificial piers, these laboratory models investigated structural flow collars as deflectors in pier design for which the results are as follows.

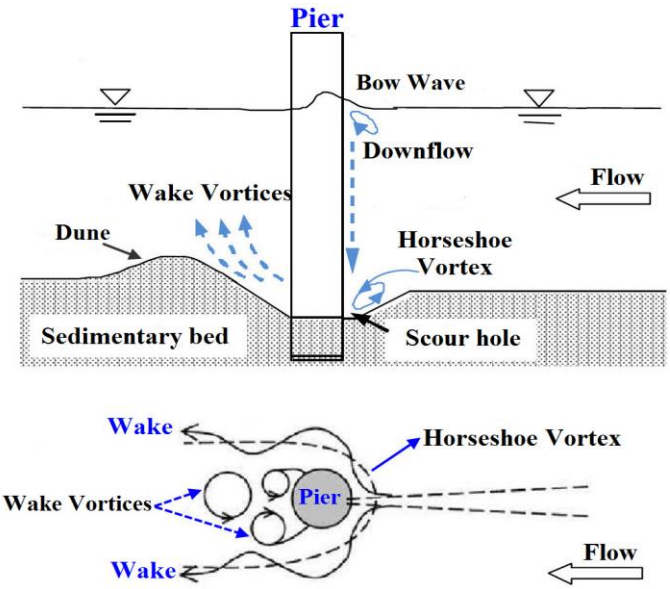

Fig.1- Flow around a circular pier in a scour hole

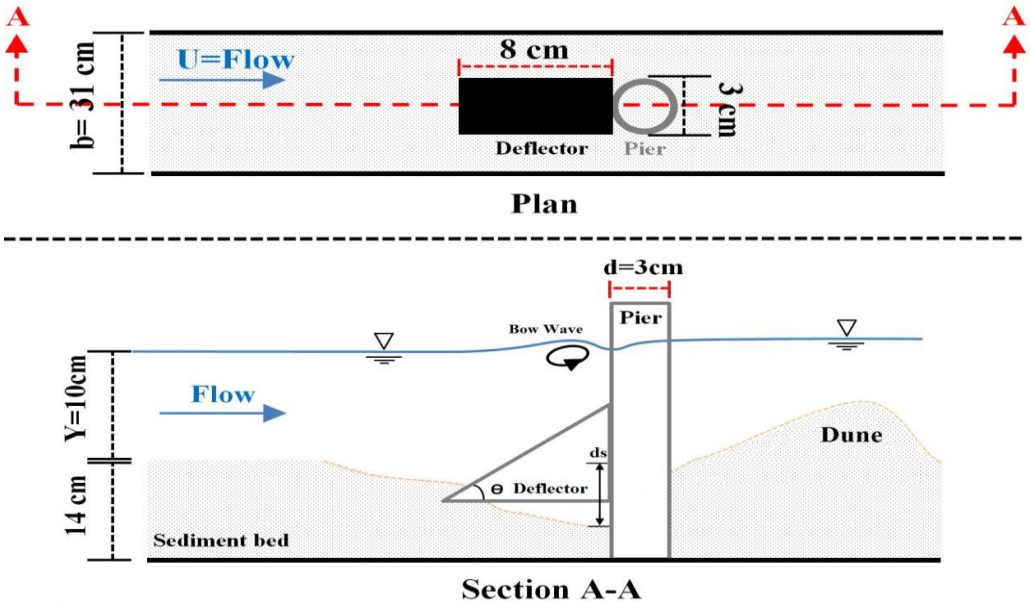

Fig. 2. Plan and section of the setup

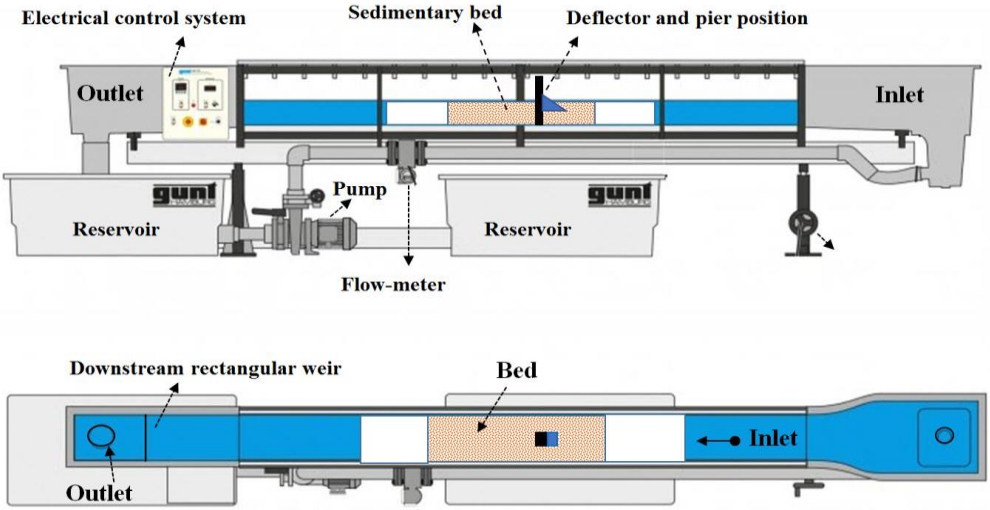

Fig. 3-Definition sketch of the testing flume

Materials and Methods

Dimensional Analysis

The important parameters to investigating the effect of deflector structure on bridge pier scour are shown according to Equation (1).

$$F_1(d, d_0, D_S, d_s, d_{s_{max}}, y, U, U_c, g, \rho, \mu, b, \Theta)=0 \quad (1)$$

In this equation, d is the cylindrical pier diameter, d_0 is the square pier width, D_s is the sediment particle diameter, d_s is scour depth, $d_{s_{max}}$ is the control cylindrical and square pier's scour depth, y is the flow depth, U is the flow velocity, U_c is the sediment incipient motion velocity, g is the gravity acceleration, ρ is fluid density, μ is water viscosity, b is flume width, and Θ is the angle of the deflector structure. By applying the Buckingham's dimensional analysis method and assuming ρ, U, d as duplicate variables, this equation can be written as the following dimensionless function:

$$F_2(Re, Re_c, Fr, Fr_c, \frac{d_s}{d}, \frac{U}{U_c}, \frac{y}{d}, \frac{d}{d_{50}}, \frac{b}{d}, \Theta)=0 \quad (2)$$

According to Rajaratnam and Ahmed (1998), since the Reynolds number (Re) in this equation exceeded 3000 for all experiments, the flow is completely turbulent, and the viscosity effect can be neglected. Due to the subcritical flow in all experiments and its small range, the $(\frac{U}{U_c})$ relative velocity was used instead of the Froude number (Fr) for graph analysis and interpretation. Since b, D_S, d_0, and y were constant for all experiments. These parameters can also be disregarded, and Equation 3 can be written as follows:

$$F_3(\frac{d_s}{d}, \frac{U}{U_c}, \Theta)=0 \quad (3)$$

Or

$$\frac{d_s}{d} = F4(\frac{U}{U_c}, \Theta) \quad (4)$$

In Equations 3 and 4, $(\frac{d_s}{d})$ is the relative scour depth $(\frac{U}{U_c})$ is the relative velocity, and (Θ) is the deflector structure's angle relative to the flow direction. (Figure 2).

Laboratory setup

The tests were conducted in a Gunt research flume located in the Hydraulics and Fluid Laboratory of the KWPA Research and Educational Center. Figure (3) shows the flume's specifications in a schematic. The flume shown in the image is 10 meters long, 31 centimetres wide, and 50 centimetres high. The frame of the flume was metal, and its walls were glass, which allowed for observing the channel's flow and other phenomena. A resting basin was placed at the flume inlet to prevent flow turbulence; a rectangular spillway placed at the flume basin's outlet was used for adjusting water level inside the flume. The water supply was circulating and allowed for continuous experiments. A pump with a maximum flow of 51 lit/sec was used for flume water supply. The pump inlet was controlled with a bypass

 DOI: 10.22055/jise.2021.36337.1950.

valve, and an electromagnetic flowmeter was used for measuring the inlet flow with an accuracy of ±0.1 lit/sec. The experiments were taken in a 2m-long rectangular section at a 3-meter distance from the channel inlet.

Experimental set-up

A. Model dimensions

The first step for doing the tests was to determine the model's dimensions as well as the permissible variables affecting maximum scour depth; the useful parameters were selected from the assortment of factors by previous researchers to create a condition for maximum local scour depth. The secondary effect of flume walls on scour depth should be considered in selecting the pier model width and diameter. According to Raudkivi and Ettema (1983), the ratio of the pier size to channel width should not exceed 0.16. based on Melville (1997) recommendations, that pier diameter should not exceed 10% of the flume's width. Considering the 31 cm flume width and the criteria, the cylindrical Teflon pier and the square PVC pier were used both having a 3 cm diameter. PVC deflector structures with the same width as piers, 8 cm length, and 15-, 30-, and 45-degree angles were designed and built.

B. Sediment size

The sediment particle diameter (D_S) should provide maximum scour depth around the bridge pier, while leaving the equilibrium scouring depth unaffected by sedimentary particles size (Melville, 1997). Lee and Sturm (2009) have stated the minimum d/d_{50} to be 25 (d is the pier diameter or width and d_{50} is the mean sedimentary particles size). In this study, this ratio is 31.57. According to Raudkivi and Ettema (1983), the average sedimentary particle size should be over 0.7 mm to prevent ripple formation. Therefore, the mean particle size (d_{50}) was set to 0.95 mm to obtain maximum scour while preventing ripples. This study used natural riverbank sand with a relative density of $G_s = 2.64$ and a mean particle diameter of 0.95 mm. The sediment's geometric deviation of $\delta_g = 1.36$ was calculated according to Equation (5)

$$\delta_g = \sqrt{\frac{d_{84}}{d_{16}}} \quad (5)$$

where d_{84} and d_{16} respectively represent a particle size larger than 84% and 16% of particles, which is smaller than 1.5 and meets Hassanzadeh et al (2018) uniformity criterion.

C. Selection of flow depth and velocity

Flow depth and velocity affect the final scour depth if they are selected incorrectly. According to Chiew (1995) and Ettema (1980), to avoid the effects of flow depth on scouring pattern, it should be three times greater than the pier diameter or width (y>>3×d). Melville and Chiew (1995) argued that the maximum shear stress should be investigated in clear water to determine the flow depth. When the mean velocity is in the range of $0.3U_c < U < U_c$, it indicates the scour in clear water, and live-bed scour occurs when the mean velocity (U) exceeds the critical velocity. In this research, the experiments were designed around the clear-water scour condition. Likewise, the experiments were conducted in the clear-water condition. Hence, to determine incipient motion velocity, the computational method and laboratory observations were used. The mean size of bed quartz particles was determined in 20 °C water, and Melville's equations provided a good estimation of the Shields curve.

$$U_{*_c} = 0.0115 + 0.0125 d_{50}^{1.4} \rightarrow (FOR \rightarrow 0.1mm < d_{50} < 1mm) \quad (6)$$

$$U_{*_c} = 0.305 d_{50}^{0.5} - 0.0065 d_{50}^{-1} \rightarrow (FOR \rightarrow 1mm < d_{50} < 100mm) \quad (7)$$

The logarithmic velocity distribution equation was used for critical velocity:

$$U_c = 5.75 \log\left(5.53 \frac{y}{d_{50}}\right) \times U_{*_c} \quad (8)$$

According to these equations, the sediment incipient motion velocity was 0.183 m/s. Experiments without the pier, constant depth and various velocities were used to determine the incipient motion velocity and

record the particle movement conditions. The average of recorded velocities resulted in the incipient motion velocity of 0.22 m/s using Armfield-Streamflo Velocity Meter Figure (4) with the ability to measure velocities as low as 5.0 cm/sec. According to these criteria and the calculated sedimentary particle incipient motion velocity, the $\frac{U}{U_c} = 0.97$ condition was established with a constant 10cm flow depth. Assuming $\frac{U}{U_c} = 0.97$, all scenarios can be compared in identical conditions close to the bed sediment incipient motion.

D. Time duration of experiments

According to Kumar et al. (1999) for time duration of experiments, an equilibrium time is the time in which scour depth changes does not exceed 1 mm in three times of testing consecutively. Therefore, a long, 12-hours experiment was conducted on the control pier test in the critical flow condition ($\frac{U}{U_c} = 0.97$), cylindrical and square piers sections, without deflector. Figure 5 suggests that the scour depth changes after almost 480 minutes is below 1 mm with a 98% scour. Therefore, the equilibrium time in all the experiments was considered to be 8 hours.

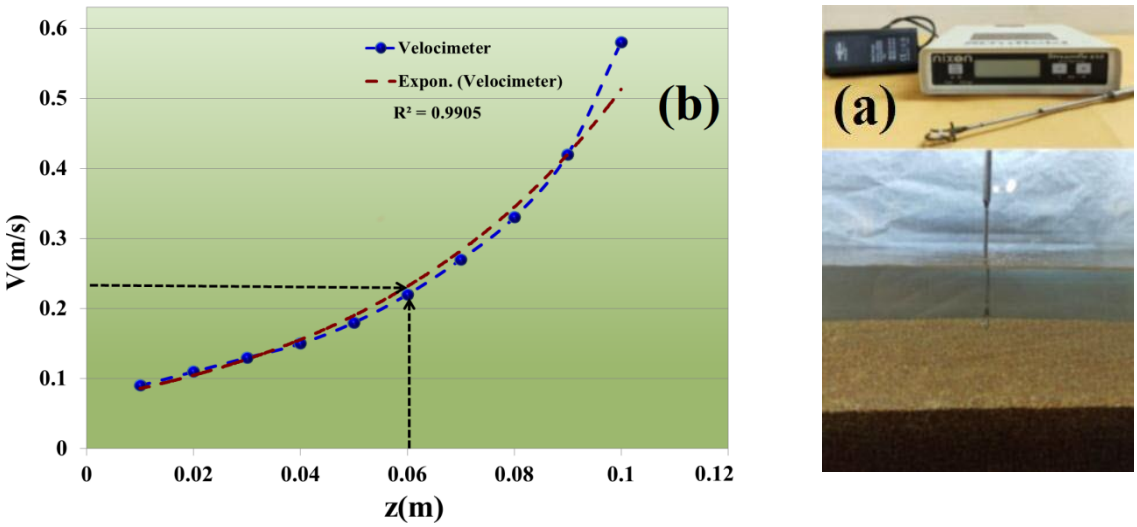

Fig. 4- (a) Armfield-Streamflo Velocity Meter, and (b) velocity meter's graph

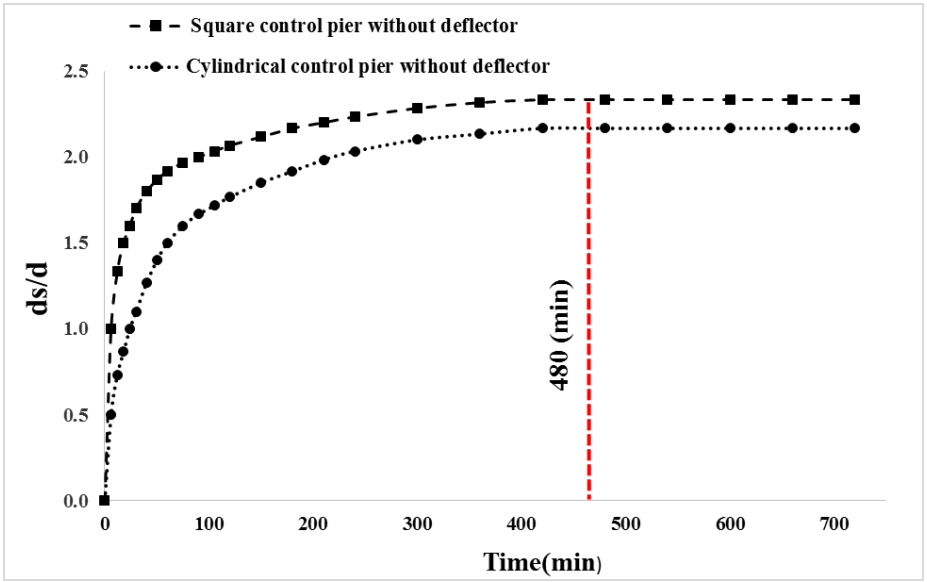

Fig. 5- Time variations of scour depth

 DOI: 10.22055/jise.2021.36337.1950.

The pier protection solutions against scour introduced so far target the scour reduction and control mechanism by changing the flow pattern around the pier either directly with bed armouring or indirectly by changing the flow pattern around the pier. This study introduced a structure and set the experiment scenarios accordingly to cover both protections as the deflector to reinforce the bed and modify the flow pattern to divert flow toward the bed. Two cross-sections (square and circular) for piers were considered to investigate the effect and interaction between the deflector and pier shape.

Models Specifications

This study used cylindrical and square piers with 3 cm diameter and width, 30 cm height, and three deflectors with 15-, 30-, and 45-degree angles. Figure (6) shows the model's pacification.

The scour depth reduction percentage in Equation 9 was used for evaluating the deflector's effect on scouring:

$$R\%=\left(\frac{d_s - d_{smax}}{d_{smax}}\right)\times 100 \quad (9)$$

where ds and dsmax respectively represent the scour depth and the equilibrium scour depth. Table (1) shows the flow conditions governing the experiments, and Table (2) shows the experiment components according to the scenarios.

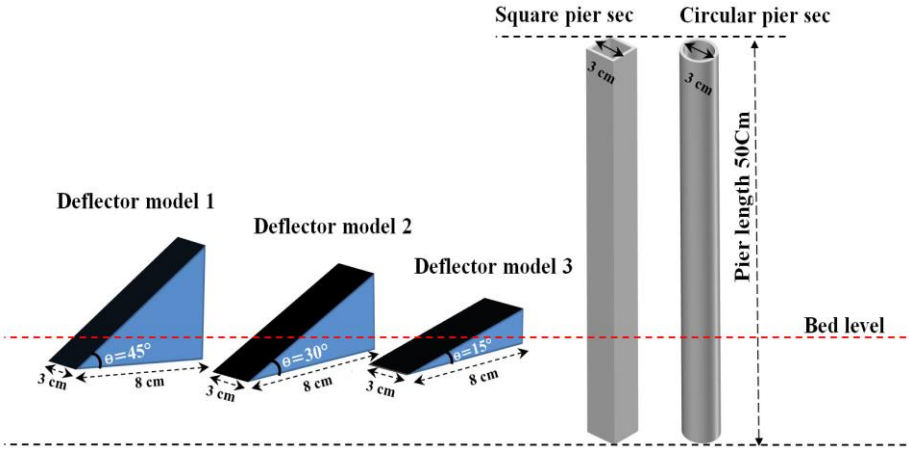

Fig. 6- Sketch of deflectors and piers models

Table 1- Summery of experimental hydraulics conditions

Flume width (Cm)	Square pier width (Cm)	Circular pier diameter (Cm)	Mean particles size (mm)	Water depth (Cm)	Water discharge (m^3/h)	Relative velocity	Reynolds	Froude
B	d	d	d_{50}	Y	Q	U/U_c	Re	Fr
31	3	3	0.95	10	21<Q<29	0.70<U/Uc<0.97	>20000	0.32<Fr<0.45

Table 2- Details of experiments

Row	Models	Deflector's angle	Relative velocity	Dimensionless relative depth	Scour reduction Percentage
Test	Pier's name	θ	$\frac{U}{U_c}$	$\frac{d_s}{d}$	$\frac{d_s}{d}\%$
1	Circular pier	15°	0.70	0.20	90
2	Circular pier	15°	0.83	0.37	82
3	Circular pier	15°	0.97	0.50	75
4	Circular pier	30°	0.70	0.27	85
5	Circular pier	30°	0.83	0.43	75
6	Circular pier	30°	0.97	0.70	58
7	Circular pier	45°	0.70	0.30	77
8	Circular pier	45°	0.83	0.50	67
9	Circular pier	45°	0.97	0.83	40
10	Square pier	15°	0.70	0.40	89
11	Square pier	15°	0.83	0.63	81
12	Square pier	15°	0.97	1.03	70
13	Square pier	30°	0.70	0.47	83
14	Square pier	30°	0.83	0.67	73
15	Square pier	30°	0.97	1.20	56
16	Square pier	45°	0.70	0.63	73
17	Square pier	45°	0.83	0.83	64
18	Square pier	45°	0.97	1.50	36
19	Cylindrical control pier	without deflector	0.97	2	-
20	Square control pier	Without deflector	0.97	2.33	-

Results and discussion

Experiments

A) Un-protected Pier Test (Control tests)

The un-protected control pier scouring was investigated first to represent a basis for controlling and comparison with the other scour and bed changes conditions. As mentioned earlier, a 12-hour control experiment was conducted on the control pier to determine the experiment time (equilibrium time), and changes in scour depth were recorded in the time unit during the experiments. The results of the control tests showed that water flow's contact with the pier immediately created vortexes around the cylindrical pier due to down flow, that the scour process starts at a high-speed rate, and that horseshoe vortexes start around the pier as the hole depth increases. The sediments raised from the hole are transferred downstream and accumulated on both sides behind the pier with near symmetry to form a sedimentary ridge. Sometime after the experiment began, the sediments were lifted from the scour hole to reach a level that decreased the pier's effect on the area, and the impact of vortexes behind the pier became negligible. In this condition, the

sediments transferred from the scour hole were affected by the secondary downstream flow, and after 8 hours, the scour rate decreased significantly. Scour depth at the front of the pier was also at the maximum, and its degree around the pier decreased at higher proximities. Figure (7) shows the hole formation and the scour sedimentary ridge in the cylindrical and square pier models. The longitudinal bed profiles were used next for comparison. The figures and bed profiles suggest that the deflector changes the flow pattern around the pier.

B) Deflector structure tests

Figures (8) and (9) show the longitudinal scour profile for square and circular cross-section piers for various deflector angles in $\frac{U}{U_c} = 0.97$. In both models, the lower deflector angle also decreases the scour depth. Moreover, the lower deflector angle decreases the scour depth around the deflector structure itself. The figures show that the presence of the deflector structure in front of the pier diverts the flow lines near the bed to the upper layers and reduces scour. Simultaneously, changing the deflector angle relative to flow lines and increasing it from 15 to 45 degrees leads to different structural behaviour. As shown, increasing the deflector angle increases the scour depth, which will explain the phenomenon in more detail.

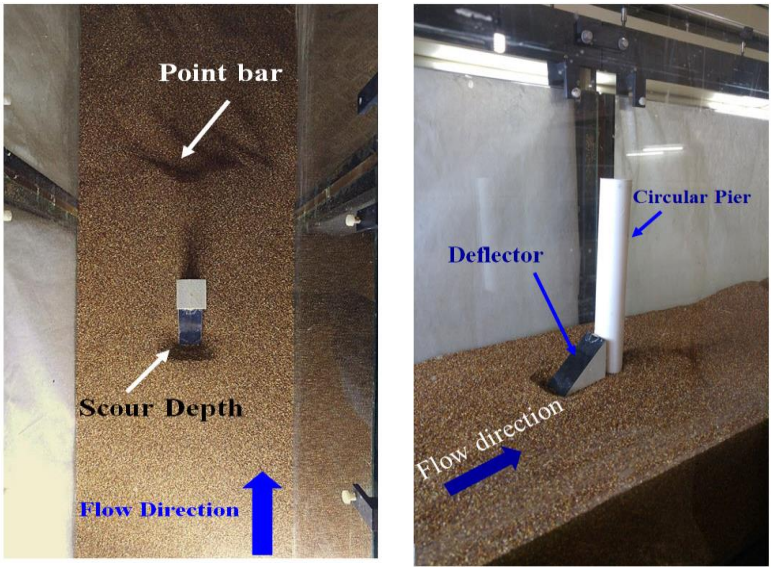

Fig. 7- Photos of experimental tests

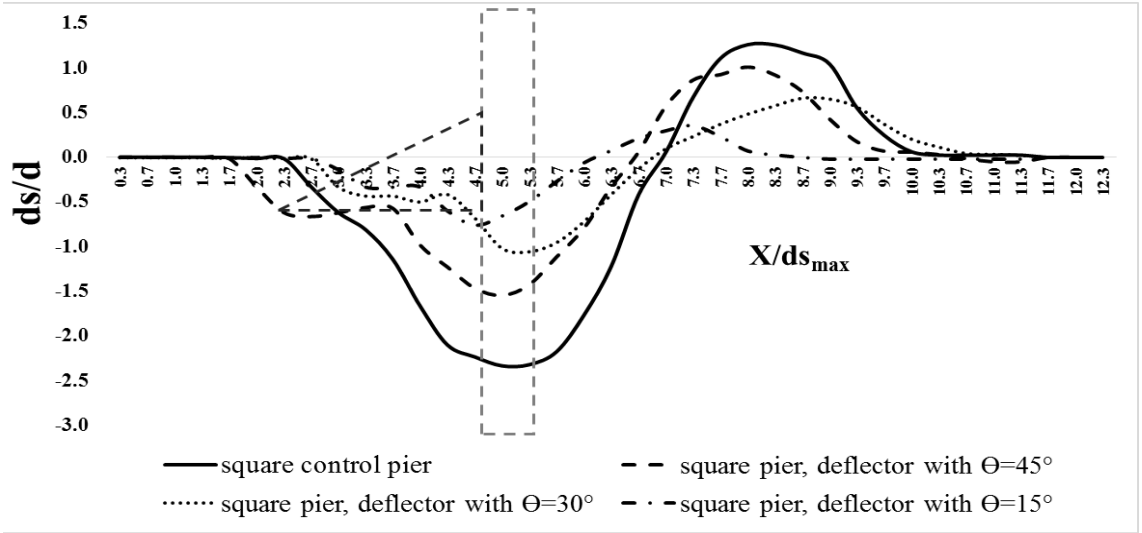

Fig. 8- Longitudinal profiles of piers with square cross-section

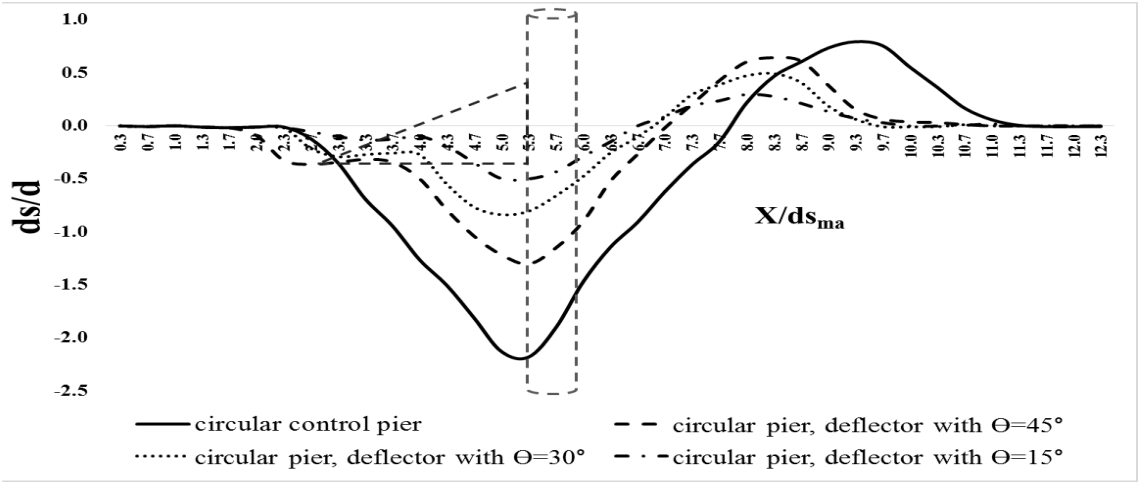

Fig. 9- Longitudinal profiles of piers with circular cross-section

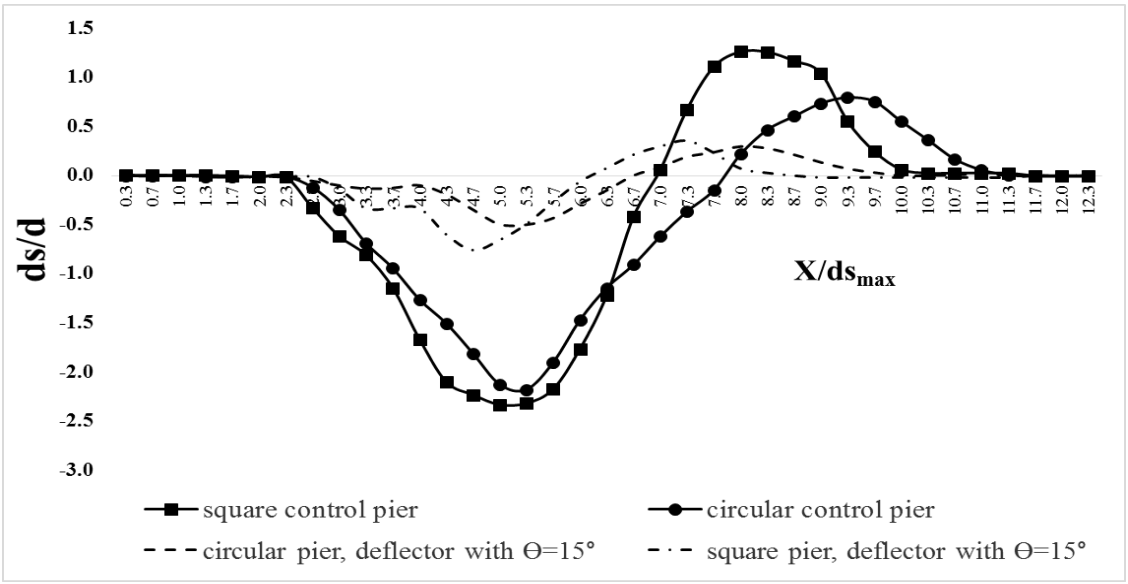

Fig. 10- Comparison of different scenarios, control tests and piers protected by deflector with θ =15°

Figure (10) shows a more accurate investigation of pier cross-section transformation and its interaction with the deflector structure. This figure shows the best protective structure or $\Theta = 15°$ as shown in Figures 8 and 9. According to this figure, combining the deflector structure with the circular pier results in better conditions than those in the square cross-section, In contrast, both systems lead to significant reductions compared to the control states. The quantitative graphs of scour depth reduction will be shown as follows. Although both cross-sections have no significant functional differences based on the graph, the negligible difference is due to the circular cross-section and its lower flow resistance.

Figures (11) and 12 show the quantitative scour depth reduction for the scenarios defined in the experiments. In these figures, each structure is exposed to three dimensionless $\frac{U}{U_c} = 0.97, 0.83, 0.70$ relative velocity parameters to evaluate the effect of the $(\frac{U}{U_c})$ relative velocity on flow conditions and scour. According to Figure 11, the deflector with a $\Theta = 15°$ in front of the circular pier reduces the dimensionless scour parameter $(\frac{d_s}{d})$ by 90% in the $\frac{U}{U_c} = 0.70$ relative velocity, which reaches 75% by

 DOI: 10.22055/jise.2021.36337.1950.

increasing the flow velocity to the incipient motion and is very significant for scour depth reduction around the pier. Increasing the angle from 15 to 30 and 45 degrees in the incipient motion conditions decreases the value to 45 and 40%, which shows that changing the deflector's angle and increasing the θ reduces the deflector's effect and increases the scour depth relative to the θ = 15° angle.

Figure (12) shows the conditions for the square pier. This figure, which is an iteration of the previous state but with a square section, has similar conditions, and the deflector with the θ = 15° provides the best response in reducing the scour depth. According to Figures 9 and 10, the 2 to 5% difference between the square and circular cross-sections in identical conditions suggests minor variation in scour conditions, which means that the deflector protects the pier regardless of cross-section type.

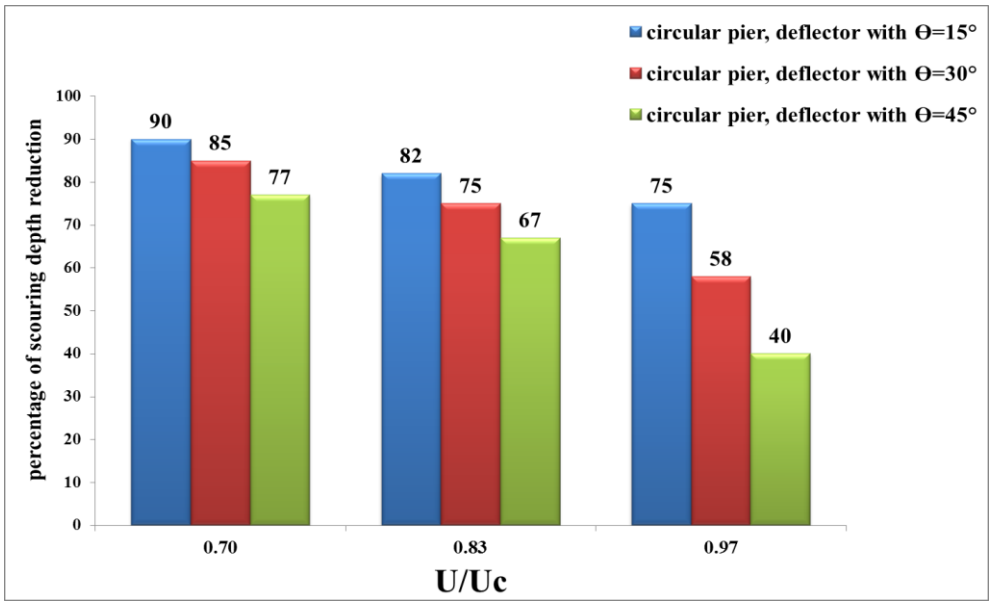

Fig. 11- Percentage of scouring depth reduction relative to control test for circular pier

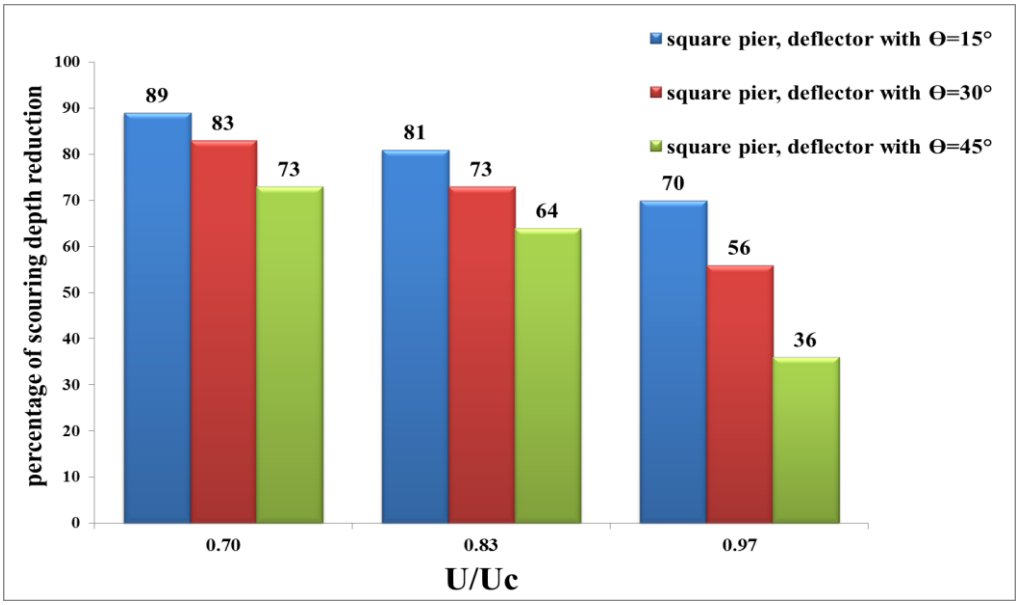

Fig. 12- Percentage of scouring depth reduction relative to control test for square pier

Figures (13) and 14 show the changes of scour depth dimensionless parameter ($\frac{d_s}{d}$) against the dimensionless relative velocity parameter ($\frac{U}{U_c}$) for all the experimental scenarios. These figures demonstrate the deflector's effect in reducing the scour depth and at the same time illustrate that the slope of the velocity change graph in the $\theta = 15°$ state is constant. Contrary to the control state near the incipient motion, the slope does not change. Simultaneously, this uniformity shows that the deflector structure with $\theta = 15°$ steadily diverts the flow lines near the bed upwards, weakens the down flows, and disrupts the flow deflection mechanism toward the bed, leading to a decrease in the energy of horseshoe vortexes

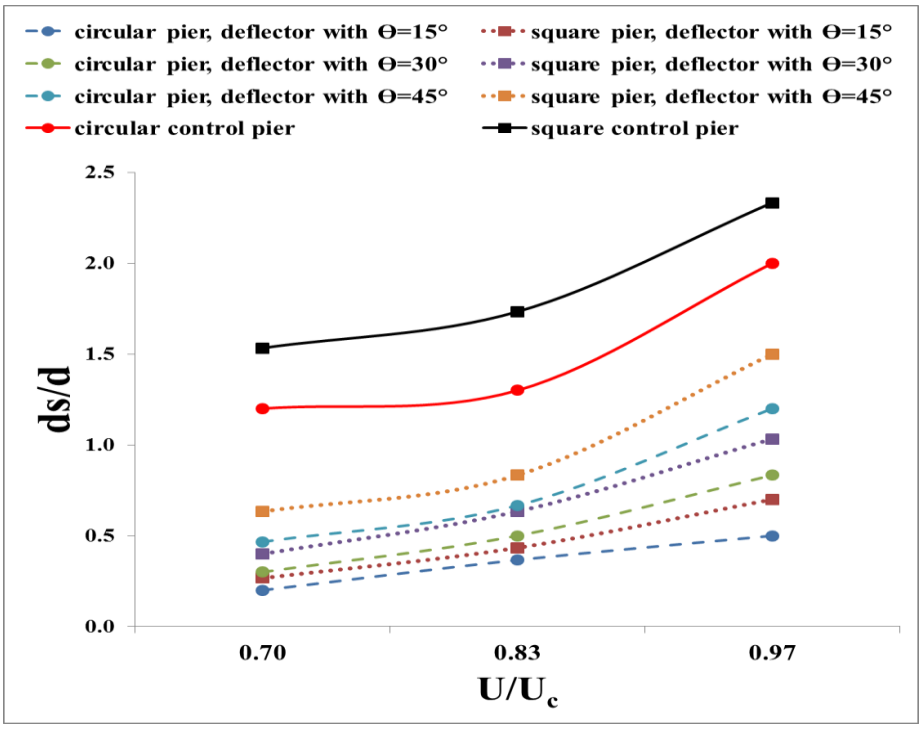

Fig. 13- Dimensionless scouring depth for all scenarios against relative velocity

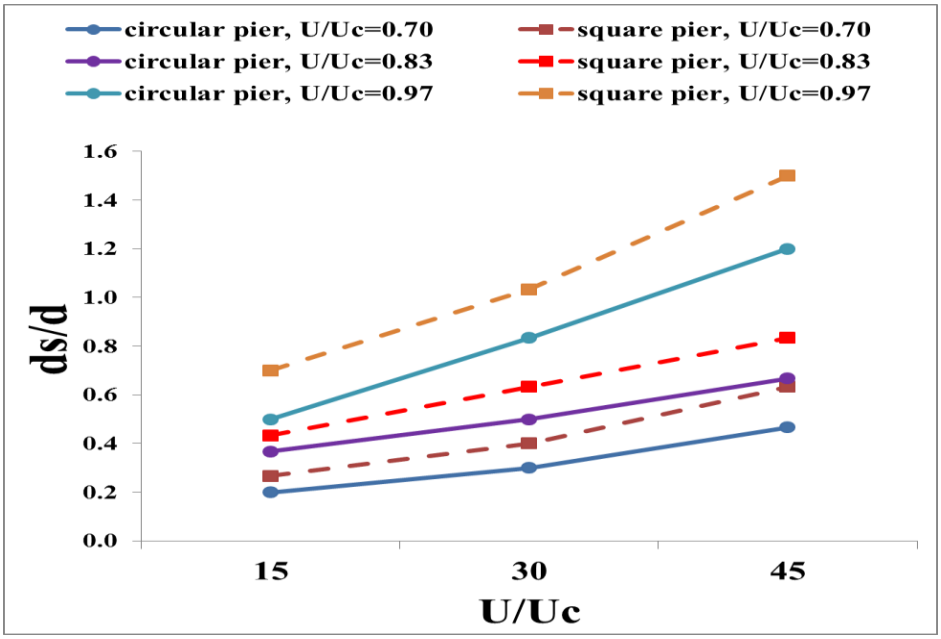

Fig. 14- Dimensionless scouring depth for all scenarios against the deflector angle

Conclusion

This study used a deflector structure to reduce and control the scour depth around bridge piers. The flow effect was investigated by implementing these protections and their effect in various relative velocities ($\frac{U}{U_c}$). The square and circular cross-sections were investigated to study the impact of pier shape on protection, and the results are as follows:

1. Combining the deflector structure with the circular pier provides superior results compared to the square cross-section due to its lower flow resistance. In contrast, both structures show significant reductions compared to the control conditions.

2. In the best case scenario with the deflector at the 15-degree wedge angle relative to the flow direction in near incipient motion conditions ($\frac{\mathrm{U}}{\mathrm{U_c}} = 0.97$), the dimensionless scour ratio ($\frac{d_s}{\mathrm{d}}$) was 70% for the square cross-section pier and 75% for the circular cross-section pier.

3. Increasing the deflector wedge angle from 15 to 45 degrees increases the structural resistance against the flow and scour depth. the scour depth reduction percentage decreases from 70% to 36% for the pier with the square cross-section, and from 75% to 40% for the pier with the circular cross-section.

4. The differences between the square and circular cross-sections in identical conditions is 2 to 5%, which is a negligible difference in scouring conditions and means that the deflector protects the pier regardless of cross-section type.

5. Changing the flow condition and the dimensionless relative velocity parameter's effect ($\frac{\mathrm{U}}{\mathrm{U_c}} = 0.97, 0.83, 0.70$), and investigating the flow effect on structural scour indicates that the scour depth with the deflector at 15 degrees has a linear and constant slope as a result of increasing relative velocity in steps. In the 45-degree structure, however, the decrease in the scouring depth is sudden due to the near incipient motion velocity.

6. The results state that the deflector at the 15-degree angle significantly affects the flow deflection near the bed, corrects the flow pattern around the pier, and reduces scour depth.

References

1- Abousaeidi, Z., 2018. Experimental investigation of the effect of debris accumulation on the local scour at bridge pier and abutment. *Journal of Water and Soil Conservation*, *25*(2), pp.267-282. (In Persian).

2- Adib, A., Shafai Bejestan, M. and Shiri, V., 2019. On the Local Scour Around Group Piers in Series by Experimental Tests. *Journal of Rehabilitation in Civil Engineering*, *7*(1), pp.21-34.

3- Akhlaghi, E., Babarsad, M.S., Derikvand, E. and Abedini, M., 2020. Assessment the effects of different parameters to rate scour around single piers and pile groups: a review. *Archives of Computational Methods in Engineering*, *27*(1), pp.183-197.

4- Chiew, Y.-M. 1995. Mechanics of riprap failure at bridge piers. *Journal of hydraulic engineering*, 121**,** 635-643

5- Ettema, R. 1980. Scour at bridge piers.

6- Gohari, S. and Rezaei, M. 2020. Investigating the effect of oblique bed sill on bridge pier scouring with circular cross-section. *Journal Management System*, 12**,** 100-114. (In Persian).

7- Kayatürk, Ş.Y. 2005. Scour and scour protection at bridge abutments.

8- Kumar, V., Raju, K.G.R. and Vittal, N., 1999. Reduction of local scour around bridge piers using slots and collars. *Journal of hydraulic engineering*, *125*(12), pp.1302-1305.

9- Lee, S.O. and Sturm, T.W., 2009. Effect of sediment size scaling on physical modeling of bridge pier scour. *Journal of hydraulic engineering*, *135*(10), pp.793-802.

10- Melville, B.W., 1997. Pier and abutment scour: integrated approach. *Journal of hydraulic Engineering*, *123*(2), pp.125-136.

11- Melville, B.W. and Chiew, Y.M., 1999. Time scale for local scour at bridge piers. *Journal of Hydraulic Engineering*, *125*(1), pp.59-65.

12- Nohani, E. and Ebrahimi, S., 2019. Experimental Investigation of the Collar and Vanes on Reduction the Scour Depth of Cylindrical Piers. *Iranian Journal of Soil and Water Research*, *50*(2), pp.411-424. (In Persian).

13- Raeisi, N. and Ghomeshi, M. 2020. Laboratory investigation of flow pattern and scour around bridge with netted unsymmetrical collar. *Journal of Hydraulics,* 15**,** 113-128. (In Persian).

14- Rajaratnam, N. and Ahmed, F. 1998. Flow around bridge piers. *Journal of Hydraulic Engineering*, 124**,** 288-300

15- Raudkivi, A. 1998. Loose boundary hydraulics. 4th edi-tion. *Balkema, Rotterdam, The Netherlands,*

16- Raudkivi, A.J. and Ettema, R. 1983. Clear-water scour at cylindrical piers. *Journal of hydraulic engineering*, 109**,** 338-350

17- Choramin, M., Safaei, A., Khajavi, S., Parmoon, A.A. and Arezoo, A.A., 2015. Analyzing the affective parameters on the amount of bridge scour in the vicinity of the rough collar in laboratory model.

18- Hassanzadeh, H., Bajestan, M.S. and Paydar, G.R., 2018. Performance evaluation of correction coefficients to optimize sediment rating curves on the basis of the Karkheh dam reservoir hydrography, west Iran. *Arabian Journal of Geosciences*, *11*(19), pp.1-9. (In Persian).

19- Shahsavari, H., Moradi, S. and Khodashenas, S., 2020. Influence of Semicircular Collar Diameter and Its Alignment on Scour Depth and Flow Pattern around Bridge Abutment. *Iranian Journal of Soil and Water Research*, *51*(1), pp.77-91. (In Persian).

20- Vaghefi, M. and Meraji, S. 2019. The effect of 20% reduction in overlapping length of the upstream submerged vanes of bridge pier on bed topography in sharp 180 degree bend. *Modares Civil Engineering journal,* 19**,** 41-55. (In Persian).

21- Wang, L., Melville, B.W., Shamseldin, A.Y. and Nie, R., 2020. Impacts of bridge piers on scour at downstream river training structures: submerged weir as an example. *Water Resources Research*, *56*(4), p.e2019WR026720.

22- Zomorodian, S.M.A., Ghaffari, H. and Ghasemi, Z., 2019. Comparison of Linear and Triangular Arrangements of Submerged Sacrificial Piles on Local Scour Depth around Cylindrical Bridge Piers. *Irrigation Sciences and Engineering*, *42*(4), pp.167-180. (In Persian).